

Available online at www.sciencedirect.com

ScienceDirect

journal homepage: www.elsevier.com/locate/dental

Chlorhexidine-loaded poly (amido amine) dendrimer and a dental adhesive containing amorphous calcium phosphate nanofillers for enhancing bonding durability

Xue Cai, Xiaoyan Wang*

Department of Cariology and Endodontology, Peking University School and Hospital of Stomatology, Beijing 100081, China

ARTICLE INFO

Article history:

Received 17 January 2022

Received in revised form 24 March 2022

Accepted 1 April 2022

Keywords:

PAMAM dendrimer

Chlorhexidine

Amorphous calcium phosphate

Bonding durability

Matrix metalloproteinases

ABSTRACT

Objective: A novel method of combining chlorhexidine (CHX) loaded poly (amido amine) (PAMAM) dendrimers with a dental adhesive containing amorphous calcium phosphate (ACP) nanofillers are proposed for etch-and-rinse bonding system to enhance resin-dentin bonding durability.

Methods: The CHX-loaded PAMAM and ACP nanofillers were synthesized and characterized. Their effects on the cytotoxicity were tested by MTT assay. Micro-tensile bond strength (μ TBS) before and after thermomechanical challenges were used to evaluate the bonding durability. Anti-matrix metalloproteinase (MMPs) property was examined using in-situ zymography. A double-fluorescence technique was used to examine interfacial permeability after bonding. Dentin remineralization in Ca/P lacking solution was observed under scanning electron microscopy.

Results: Compared with a 0.2 wt% CHX solution, the PAMAM loaded CHX had less cytotoxicity, while the in situ zymography showed it could still inhibit MMPs activity within the hybrid layer after released from PAMAM. The application of the novel method maintained the μ TBS better than the control group after thermomechanical challenges, and it did not negatively affect water permeability of the bonding interfaces. CHX-loaded PAMAM regulated the calcium (Ca) and phosphate (P) ions provided by the ACP-containing adhesives to remineralize the demineralized dentin surfaces without initial Ca/P in the environment.

Significance: The novel method can reduce the cytotoxicity of CHX, inhibit MMPs activities, maintain μ TBS, and induce dentin remineralization, which are crucial factors for enhancing bonding durability.

© 2022 The Academy of Dental Materials. Published by Elsevier Inc. All rights reserved.

* Corresponding author.

E-mail address: wangxiaoyanpx@163.com (X. Wang).

1. Introduction

The instability of resin-dentin bonding interfaces is a major issue in adhesive dentistry [1]. Hybrid layers created by contemporary adhesives are unstable in aqueous environments because of hydrolysis of the adhesive resins and degradation of demineralized collagen matrices [2,3]. Resin monomers cannot completely infiltrate the demineralized dentin, leaving the exposed collagen fibrils at the bottom of the hybrid layer unprotected and providing an aqueous environment for degradation of collagen and leaching of enzyme degradable resinous components [4]. During the acid-etching phase of the bonding procedure, endogenous proteases, such as matrix metalloproteinases (MMPs) and cysteine cathepsins that are trapped by apatite crystallites, become exposed and activated by acidic etchants [5]. The subsequent application of resin monomers further promotes protease activities, in either the etch-and-rinse mode or self-etch mode [6]. Activated MMPs and cathepsins can degrade exposed demineralized collagen fibrils within the hybrid layers [7].

Remineralization is an effective strategy for protecting the exposed demineralized collagen fibrils [8]. This procedure can eventually exclude exogenous collagenolytic enzymes and water from the resin-dentin interface [9]. To induce biomimetic remineralization of demineralized dentin, Ca and P ions must be regulated by biomimetic analogs to form hydroxyapatite. Over the last few years, poly (amido amine) (PAMAM) dendrimers have been used to simulate the function of noncollagenous proteins (NCPs) for in situ remineralization of enamel and dentin [10]. Previous studies have indicated that the 4th generation carboxyl-terminated poly (amido amine) dendrimer (G4-PAMAM-COOH) can self-assemble into a micro-ribbon structure similar to the self-assembly process of amelogenin [11]. The dendrimer can induce both intrafibrillar and interfibrillar remineralization on dentin in vitro in a relatively short time of 14 days [12]. However, biomimetic remineralization in vivo is still a time-consuming process. It is likely that demineralized collagen fibrils are already degraded by MMPs before remineralization is achieved [13]. Therefore, it is important to preserve the collagen template by inhibiting MMPs and reducing the remineralization time.

Chlorhexidine (CHX), a nonspecific MMP inhibitor, can reduce the activity of MMPs within the hybrid layers, and it has been incorporated into restorative materials [14]. As the cytotoxicity may increase with the concentration of CHX [15,16], it is necessary to balance the cytotoxicity and anti-MMP property. It has been widely accepted that CHX greater than 0.2 wt% could be effective in enhancing bonding durability [17,18]. However, 0.2 wt% CHX also has a cytotoxic effect [19]. Direct exposure even to a small amount of 0.02 wt% CHX for one minute had a negative effect on cell survival rates compared with no treatment [16]. In addition, CHX does not co-polymerize with resin monomers, eventually leaching from the polymerized resin network [20]. Therefore, the long-lasting anti-proteolytic effects may be a concern after CHX leaching.

Fortunately, G4-PAMAM-COOH is a highly branched polymer with internal cavities that have the potential for

loading guest molecules [21,22]. Additionally, the molecular weight of G4-PAMAM-COOH ($M_w = 20,615$ Da) is within the size retention range of type I collagen (6–40 kDa). The collagen network could let the G4-PAMAM-COOH infiltrate into the collagen microfibrils because of the size-exclusion features [23,24]. The G4-PAMAM-COOH then retains within the dentin by electrostatic interaction between dentin minerals and carboxylic terminations [25]. CHX-loaded G4-PAMAM-COOH has been synthesized in a previous study, and it was effective in inhibiting MMP activity in demineralized dentin [26]. However, the CHX-loaded PAMAM was not incorporated with restorative materials. The cytotoxicity and long-term effectiveness were not investigated either.

Although various agents have been used for remineralization, most are only effective in a saliva rich environment [27–30]. The constant flow of saliva had strong buffer capacity. The high concentrations of calcium (Ca) and phosphate (P) ions could help decrease the solubility of hydroxyapatite and promote tooth remineralization [31]. However, individuals with higher risks of secondary caries usually suffer from reduced saliva. Therefore, more effort is needed to achieve remineralization with a deficient supply of Ca and P ions. Nanoparticles of amorphous calcium phosphate (ACP) were mixed into adhesives in many previous studies [9,31,32]. These adhesives can release Ca and P ions, neutralizing the acidic environment and providing Ca and P ions for the remineralization procedure [33].

The objective of the present study is to propose a novel method for enhancing bonding durability, including CHX-loaded PAMAM dendrimers as a pretreatment agent and ACP nanoparticles as adhesive fillers. Their effects on the cytotoxicity, micro-tensile bond strength (μ TBS) before and after thermomechanical challenges, anti-matrix metalloproteinase (MMP) property, permeability of bonding interfaces, and dentin remineralization were investigated.

2. Materials and methods

Deionized water was produced from a Millipore system (MilliporeSigma, MA, USA). The G4-PAMAM-COOH was produced by Chenyuan Dendrimer Tech., Weihai, China. All other unspecified solvents and reagents were obtained from Sigma Aldrich, MO, USA. Extracted sound human teeth were collected with the donors' informed consent from Peking University School and Hospital of Stomatology. All teeth were stored in 0.9% NaCl at 4 °C and used within 3 months of retrieval.

2.1. Preparation and characterization of the CHX loaded PAMAM dendrimer

An excess of solid CHX acetate powder was added to a 10 mg/mL aqueous solution of G4-PAMAM-COOH. The solution was kept in a water bath sonicator (Biosonic UC100, Coltene Whaledent, OH, USA) at 37 °C for 1 h and then transferred to an orbital shaker (Liuyi, Shanghai, China) at 37 °C for 24 h. The solution was centrifuged at 4000 rpm for 10 min (5415R, Eppendorf, Germany). The clear supernatant was dialyzed against deionized water in dialysis bags with 1 kDa molecular

Table 1 – Setting of the experimental groups.

Group	Step 1 Total - etch	Step 2 Coating with pretreatment agent	Step 3 Adhesive
Control	37 wt% phosphoric acid etch for 15 s, rinsed with water and blot-dried with lint-free paper	100 μ L of deionized water for 40 min, blot dried	Two consecutive coats of PBE adhesive were applied and light cured
CHX-PAM		100 μ L of CHX-loaded PAMAM solution (10 mg/mL) and brush with an applicator tip for 40 min, blot-dried	
CHX-ACP		100 μ L of CHX solution (0.2 wt%) for 40 min, blot-dried	Two consecutive coats of experimental adhesive (20 wt%ACP + 80 wt% PBE) were applied and light cured
CHX-PAM-ACP		100 μ L of CHX-loaded PAMAM solution (10 mg/mL) and brush with an applicator tip for 40 min, blot-dried	

weight cut-off to remove unloaded CHX. The resulting conjugate was lyophilized and characterized by ^1H NMR spectrum analysis at 25 °C on a 500 MHz Advance spectrometer (Bruker, Germany). The remaining solid CHX was collected and lyophilized to calculate the drug loading.

2.2. Incorporation of ACP nanoparticles into a universal adhesive

ACP nanoparticles stabilized with polyaspartic acid (PAsp) were synthesized by mixing equal volumes of 10 mM CaCl_2 , 480 $\mu\text{g/mL}$ PAsp, and 6 mM Na_2HPO_4 . The liquid was then stirred for 10 min at room temperature. The precipitate was collected by centrifugation (15,000 rpm) and subsequently washed with deionized water and ethanol sequentially. Then, the ACP nanoparticles were dried at 30 °C in a vacuum drying oven overnight.

The morphology of ACP nanoparticles was observed by scanning electron microscopy (SEM, SU8010, Hitachi, Japan) under 10 kV, and transmission electron microscopy (TEM, JEM-1011, JEOL, Japan) under 100 kV. Dynamic light scattering measurements (DLS, Dynapro nanostar, Wyatt Technology, CA, USA) was used to analyze the particle size. The nanoparticles were suspended in deionized water at a concentration of 0.1 mg/mL. The amorphism of ACP was checked by selected area electron diffraction (SAED) and Fourier transform infrared spectroscopy (FTIR, Spectrum 400, MA, USA) in the range of wave number 4000 ~ 400 cm^{-1} .

Prime&Bond Elect (PBE, Dentsply Caulk, DE, USA) was used as the carrier adhesive. The following four groups of adhesives were made, and micro-tensile bond strength (μTBS) was tested to select a proper concentration of ACP nanofiller: (1) 100% PBE; (2) 10 wt% ACP + 90 wt% PBE; (3) 20 wt%ACP + 80 wt% PBE; (4) 30 wt% ACP + 70 wt% PBE.

The μTBS testing methods are described in Section 2.5. After testing, (20 wt%ACP + 80 wt% PBE) was selected for subsequent experiments because it was the maximum concentration that did not negatively affect the bond strength.

2.3. Ca and P ion release from the experimental adhesive

The experimental adhesive (20 wt%ACP + 80 wt% PBE) was placed in a mold and light cured for 20 s to prepare 5-mm diameter and 2-mm thick disks. Three adhesive disks were suspended in 15 mL of deionized water and then placed on a

horizontal shaker at 25 °C and agitated at 50 rpm. At selected points of time, 200 μL aliquots were removed and replaced by an equal volume of deionized water. The concentrations of Ca and P in the aliquot were analyzed using an automatic biochemical analyzer (7180, Hitachi, Japan). Released ions are reported in cumulative concentrations. The experiment was repeated three times.

2.4. Cytotoxicity

2.4.1. Dentin disk preparation

A 5 × 5 × 2 mm dentin disk was cut from each extracted tooth using a water-cooled low-speed diamond saw (Isomet, Buehler, IL, USA). The coronal surfaces were polished with 600-grit wet silicon carbide paper until all of the enamel was removed and a standardized smear layer was created.

2.4.2. Cell viability evaluation

Four groups were set in all the following experiments of the current study as described below in Table 1:

Forty extracted sound human third molars were used in cytotoxicity test (4 groups, 2 cycles, N = 5). Sterile Teflon disks were used as the negative control. A cyclic protocol was used to evaluate the viability of human dental pulp cells in case the cytotoxic components diffused sustainably [34]. Samples were added to the culture medium (1 sample/1 mL) and incubated at 37 °C for 24 h to simulate the elution of toxic components from the adhesive after immediate curing in a tooth cavity. After incubation, the eluent-containing culture medium was filtered through a cellulose acetate filter with a 0.22 μm diameter pore size and sterilized with ultraviolet light for 4 h for the cytotoxicity testing.

Dental pulp cells were collected from extracted healthy human third molars with the donors' written informed consent. The cultured cells were passaged after achieving 80% confluency. Fourth passage cells were used for the experiment. The cells were seeded in a 96-well plate at a density of 1×10^4 cells per well and incubated in 100 μL of medium per well for 24 h. The medium was then replaced with 100 μL of the eluent-containing medium. After incubation for 3 days, MTT assay was performed according to the manufacturer's instructions.

After the first testing cycle, the dentin-adhesive bonded samples were retrieved and re-immersed in the culture medium for 4 days to simulate continued diffusion of

materials from the dendrimer or cured adhesives. The same steps were repeated for the 2nd cycle. Data were expressed as the percentage of viable cells compared with the Teflon negative control, which was taken to be 100% viable.

2.5. Micro-tensile bond strength (μ TBS) test

2.5.1. Tooth preparation

The roots of the extracted teeth were removed 2–3 mm below the cemento-enamel junction with a low speed cutting saw under water cooling. A flat mid-coronal dentin surface was exposed by cutting the occlusal enamel perpendicular to the longitudinal axis of each tooth. The exposed dentin was polished with 600-grit wet silicon carbide paper until all the enamel was removed and a standardized smear layer was created.

2.5.2. μ TBS evaluation

Forty extracted human teeth were randomly divided into four experimental groups, as described in Table 1. After applying the adhesives, two 2-mm thick layers of resin composite (Clearfil AP-X, Kuraray, Japan) were placed over the bonded dentin. Specimens from each group were divided into two subgroups. One subgroup was stored in deionized water at 37 °C for 24 h for immediate bond strength tests. The other subgroup was thermomechanically challenged (TMC, 10,000 thermal cycles at 10 °C, 25 °C, and 55 °C for 1 min each; 240,000 mechanical cycles), corresponding to one year of intraoral use [35].

All the specimens were sectioned vertically into 0.9-mm thick resin-dentin slabs. The slabs were sectioned into 0.9 × 0.9 mm beams containing the resin-dentin interface in the center of the beam. The 10 longest beams from each tooth were used for bond testing. Each stick was attached to a testing jig with cyanoacrylate adhesive and stressed to failure under tension with a universal testing machine using a crosshead speed of 1 mm/min. The bonding procedure and μ TBS tests were performed by a single trained operator. All failure data were included. Statistical analysis was performed using the tooth as the statistical unit (N = 5).

2.6. In-situ zymography

Twelve extracted human teeth were prepared as described in Section 2.5.1 and they were randomly divided into the four experimental groups. In the bonding procedure, tetramethylrhodamine B isothiocyanate ($\lambda_{ex}/\lambda_{em}$ 553/627 nm) was mixed with the adhesives. After applying the adhesives, a 1-mm thick layer of resin composite (Clearfil AP-X) was placed over the bonded dentin. Then, a thermomechanical challenge was introduced using the protocol described in Section 2.5.2. Each sample was sectioned vertically into 1-mm thick slabs containing the resin-dentin interface. Two central slabs were selected and polished sequentially with 600-grit, 1200-grit, and 4000-grit wet silicon carbide papers under running water to obtain an approximately 50- μ m thick section with a highly glossy surface. 50 μ L of the substrate of the Gelatinase/Collagenase Assay Kit (EnzChek™, OR, USA) was coated on each slab and protected with a cover slip. After incubation in 100% relative humidity at 37 °C for 24 h, the substrate was hydrolyzed by gelatinase or collagenase and fragments with fluorescent ($\lambda_{ex}/\lambda_{em}$ 494/521 nm) were produced. Thus, the

activity of these enzymes could be expressed as the green fluorescence within the hybrid layer for simultaneous identification with a confocal laser scanning microscope (CLSM, LSM-780, Carl Zeiss, Germany). Three areas, each with a surface area of 84.9 × 84.9 μ m, were used for evaluation of each specimen. For consistency, one area was taken from the center of the slab. The two other areas were taken 2 mm away from the center area. For each area, twenty 350-nm thick optical sections were acquired from different focal planes. The images were stacked and processed with the ZEN 2010 software (Carl Zeiss). The activity of endogenous enzymes was expressed as a percentage of the green fluorescence area within the hybrid layer quantified using Image J software (3 areas × 2 slabs × 3 teeth, N = 18).

2.7. Water permeability of the bonded interfaces

Twelve extracted human teeth were prepared as described in Section 2.5.1. The remaining dentin thickness of each sample was 2.5 ± 0.1 mm from the pulpal horn. The bonding procedure was carried out in the four experimental groups. During the bonding procedure, each sample to be bonded was attached to a perforated Plexiglass block. The assembly was connected to polyethylene tubing, which was attached to a column of water containing blue fluorescence (Alexa Fluor™ 405, $\lambda_{ex}/\lambda_{em}$ 401/421 nm; ThermoFisher Scientific, MA, USA) 20 cm above the Plexiglass block to simulate the delivery of physiologic intrapulpal pressure [36]. Intrapulpal pressure was applied to the prepared dentin surface during the adhesive procedures and the 1-mm thick resin composite layer build-up. The set-up was left in the dark for 4 h after bonding to enable water permeation to the resin-dentin interface. Each sample was removed from the Plexiglass block and sectioned longitudinally through the center of the tooth to retrieve a 1-mm thick slab containing the water-perfused resin-dentin interface. Each slab was polished sequentially and observed using CLSM as described in Section 2.6. The image stack was also processed as described in Section 2.6. Blue fluorescence within and above the hybrid layer was quantified using Image J to represent the relative permeability of the respective resin–dentin interface (3 areas × 1 slab × 3 teeth, N = 9).

2.8. Mineralization of dendrimer treated dentin without the initial Ca or P ions

The dentin disks were prepared as described in Section 2.4.1. The step 1 and 2 were performed for the four experimental groups. The bonding surface of each sample was placed in contact with an adhesive disk prepared as described in Section 2.3 and they were completely immersed in 1 mL deionized water with 0.5 wt% chloramine-T.

The samples were stored in 37 °C for 28 days, then dehydrated, sputter coated with gold, and observed with SEM. Energy disperse spectra (EDS) was also performed to measure the Ca/P ratio of the regenerated minerals.

2.9. Statistical analysis

For each analysis, the data sets were analyzed for their normal distribution with the Kolmogorov–Smirnov test prior

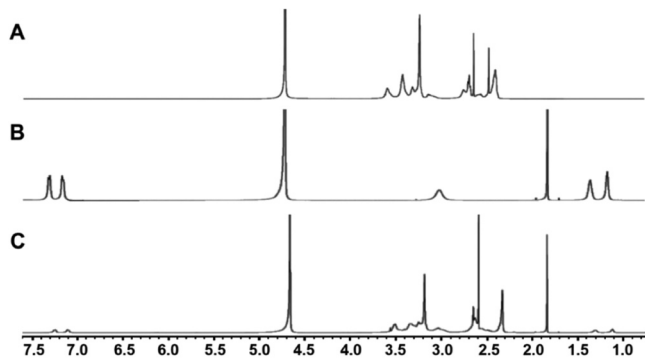


Fig. 1 – ^1H NMR spectra of (A) G4-PAMAM-COOH, (B) CHX, and (C) CHX-loaded G4-PAMAM-COOH.

to the use of parametric statistical methods. When those assumptions were violated, the respective data set was non-linearly transformed to satisfy those assumptions prior to the use of parametric statistical procedures. One-way and two-way ANOVA were applied to detect the significant effects of the variables. Post-hoc comparisons were performed using Tukey's multiple comparison. Statistical significance was set at $\alpha = 0.05$.

3. Results

Fig. 1 is the ^1H NMR spectrum of the CHX-loaded PAMAM dendrimer. Compared with the spectrum of G4-PAMAM-COOH (**Fig. 1A**) and CHX (**Fig. 1B**), the CHX-loaded G4-PAMAM-

COOH formulation (**Fig. 1C**) shows both dendrimer peaks and CHX peaks, which demonstrates a possible displacement of dendrimer protons resulting from drug inclusion and interaction. There are also slight downfield chemical shifts of these protons after complexation of CHX because of environment changes around these protons caused by the inclusion of CHX molecules. This may also indicate weak interaction between the drug and dendrimer and the formation of inclusion complexes. The calculated drug loading of CHX-loaded G4-PAMAM-COOH is $(19.56 \pm 1.27)\%$. If the CHX totally released, it would correspond to 0.2 wt% CHX solution. Therefore, the subsequent experiments in this study used 0.2 wt% CHX solution to compare.

The SEM and TEM images of PAsp (**Fig. 2A, B**) show the morphology of ACP particles. The particles have uniform, spherical forms and their diameters are smaller than 100 nm, which conforms to the standard of nanoparticles. The inset SAED pattern indicates that ACP nanoparticles remained amorphous. The distribution of the ACP particle size is shown in **Fig. 2C**. The FTIR spectrum in **Fig. 2D** also supports the amorphism of ACP. The intense peaks at 1083 cm^{-1} and 580 cm^{-1} are assigned to PO_4^{3-} . The transformation of ACP to hydroxyapatite is reportedly differentiated by the gradual splitting of the single peak at 580 cm^{-1} into two peaks at 600 cm^{-1} and 560 cm^{-1} . A mild peak at 950 cm^{-1} is also assigned to PO_4^{3-} . The peak at 1637 cm^{-1} is assigned to the O–H bending vibration [37].

Fig. 3 shows the cumulative release profiles of the experimental adhesive (20 wt% ACP + 80 wt% PBE). The light cured adhesive disks can sustainably release Ca and P ions until 28 days with faster release at the beginning.

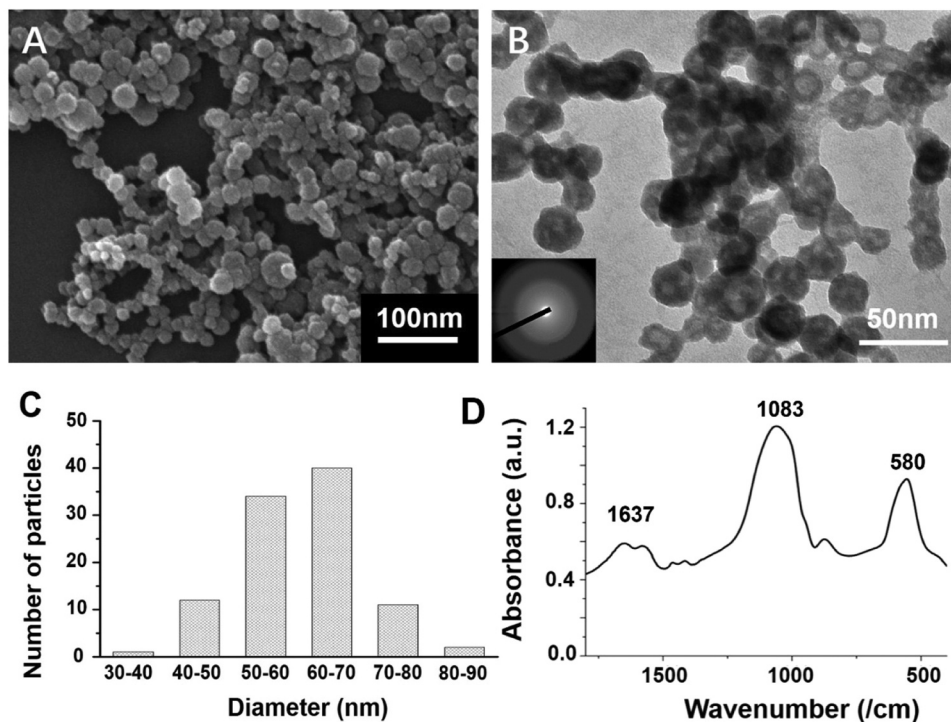


Fig. 2 – Characterization of PAsp stabilized ACP nanoparticles. (A) SEM image. (B) TEM image and SAED inset showing no diffraction patterns. (C) Particle size distribution. (D) FTIR spectrum.

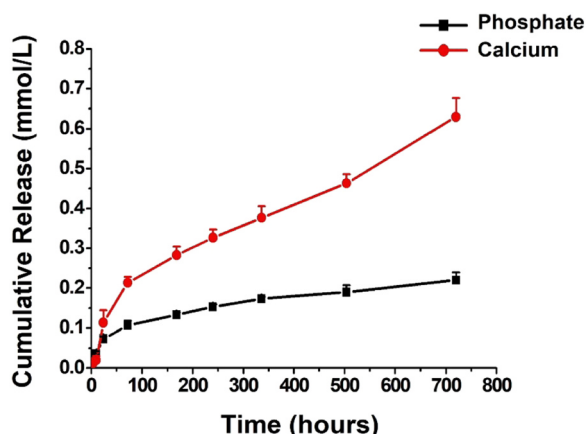


Fig. 3 – Calcium and phosphate ion release from the experimental adhesive (20 wt% ACP + 80 wt% PBE). Data are mean and standard deviation.

Fig. 4 presents the relative percentage of vital cells after incubating in the sample elution. There were significant differences among the treating methods ($P < 0.05$) and testing cycles ($P < 0.05$). The interaction of these two factors was statistically significant ($P < 0.05$). The cell viability was in the order: Teflon = Control = CHX-PAM = CHX-PAM-ACP > CHX-ACP for the 1st cycle and Teflon > Control = CHX-PAM = CHX-PAM-ACP > CHX-ACP for the 2nd cycle ($P < 0.05$). There was no significant difference between the 1st and 2nd cycle for the Teflon or CHX-ACP groups. For the Control, CHX-PAM, and CHX-PAM-ACP groups, significantly more vital cells were present in the 1st cycle ($P < 0.05$) than that in the 2nd cycle. For the CHX-ACP group, the cell viability was significantly less than the other groups in both cycles.

Fig. 5 reports μ TBS values of dentin treated with the four methods before and after TMC. The eight groups had a

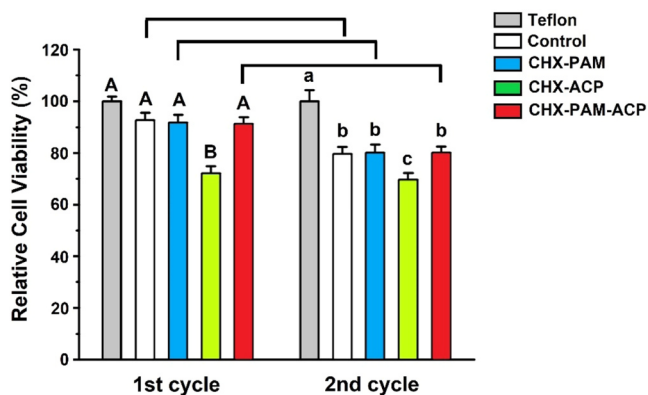


Fig. 4 – The relative percentage of vital cells. Data are mean and standard deviation. For each chart, the columns in the 1st cycle labeled with different uppercase letters are significantly different ($P < 0.05$). Columns in the 2nd cycle labeled with different lowercase letters are significantly different ($P < 0.05$). For comparison of the 1st and 2nd cycle, columns linked with a horizontal bar are significantly different ($P < 0.05$).

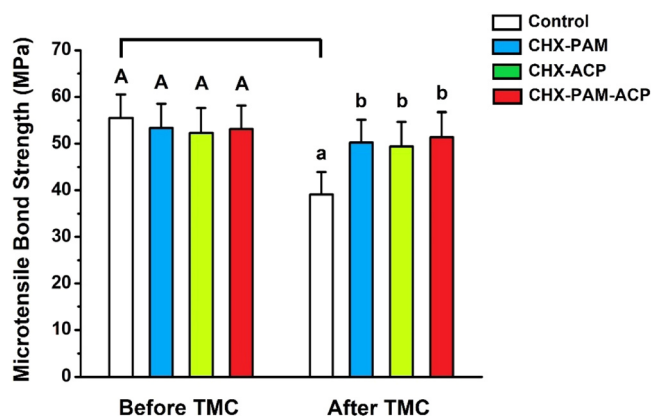


Fig. 5 – Micro-tensile bond strengths of the four groups before and after thermomechanical challenge (TMC). Values are presented as mean and standard deviation. For each chart, columns in the before TMC group labeled with the same uppercase letters are not significantly different ($P > 0.05$). Columns in the after TMC group labeled with the same lowercase letters are not significantly different ($P > 0.05$). Columns linked with a horizontal bar indicate a significant difference before and after TMC ($P < 0.05$).

similar distribution of failure modes and consisted primarily of mixed failures, with some cohesive failure in the resin composite or dentin. Similar μ TBS values were obtained in all four groups before TMC. After TMC, significantly lower μ TBS values were recorded in the Control group, while no significant difference was identified for the other three groups before or after TMC.

Representative CLSM images of in situ zymography conducted on resin-dentin interfaces treated in the four groups after TMC are shown in **Fig. 6**. Green fluorescence was indicative of hydrolysis of the fluorescence-conjugated gelatin into smaller peptides, namely the activity of endogenous MMPs. Dentin slabs prepared from the control group showed intense green fluorescence within the hybrid layers. The relative percent area occupied by green fluorescence reached $80.5\% \pm 9.6\%$. Statistically weaker green fluorescence was observed in the CHX-ACP group. The percentage of green area was $50.3\% \pm 5.4\%$. The fluorescence value in the CHX-PAM group ($20.8\% \pm 2.4\%$) and CHX-PAM-ACP group ($19.2\% \pm 2.1\%$) were even less than that of the CHX-ACP group ($P < 0.05$).

Representative CLSM images of the permeability of the resin-dentin interfaces created by the four methods are shown in **Fig. 7**. The adhesive displayed red fluorescence, and water applied with simulated pulpal pressure showed blue fluorescence. For the ideal resin-dentin interface, there should be no overlap of the two signals, which indicates water permeation into regions infiltrated by the adhesive. Water permeation was identified within the hybrid layer in all groups. However, the permeation could be limited to only the hybrid layer; no water channels or water bubbles were within or above the adhesive layer. There was no significant difference among the four groups ($P > 0.05$).

Demineralized dentin samples treated with the four methods and reacted for 28 days without initial Ca and P ions

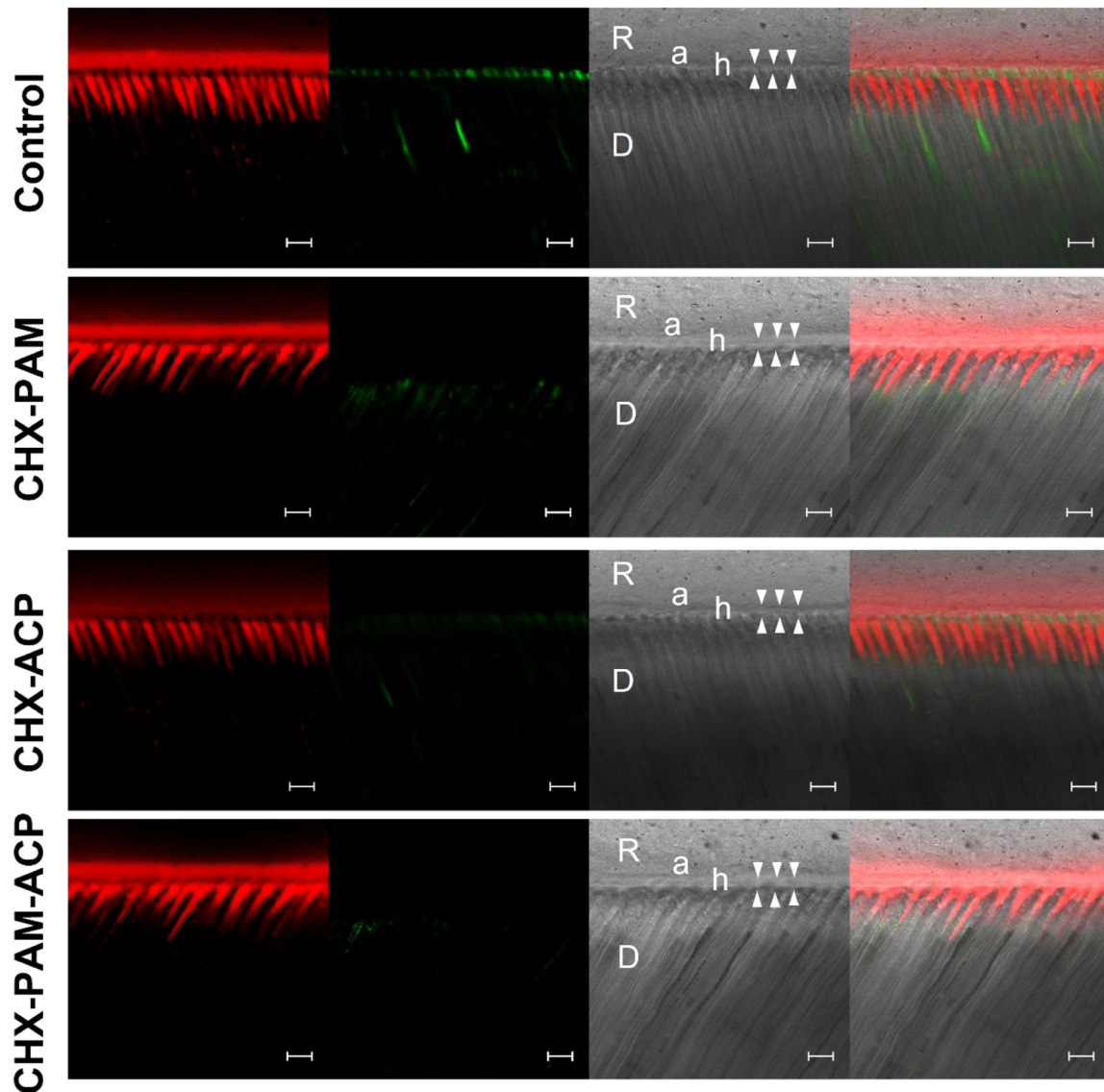


Fig. 6 – Representative confocal laser-scanning microscopy images (Bar = 10 μm) of in situ zymography conducted on resin-dentin interfaces treated in the four groups after TMC. Left: Red channel showing adhesive resin mixed with red fluorescent dye. Middle (left): Green channel showing endogenous MMPs activity caused by breakdown of fluorescein-quenched gelatin within the hybrid layer and dentinal tubules. Middle (right): Differential interference contrast images showing the optical density of the resin-dentin interface. Right: Merged channel. (R, resin composite; a, adhesive; h, hybrid layer between arrowheads; D, mineralized dentin).

are shown in Fig. 8. For the Control group (Fig. 8A1, A2), the dentinal tubules were open, and exposed collagen fibrils were thin and flexible at high magnification. For the CHX-PAM (Fig. 8B1, B2) and CHX-ACP groups (Fig. 8C1, C2), the exposed collagen fibrils were almost the same as the control. For the CHX-PAM-ACP group, needle-like crystal minerals regenerated on dentin and covered most of the dentinal tubules (Fig. 8D1). Under higher magnification, the remineralization was observed to start from the peritubular dentin in the area which was not heavily mineralized (Fig. 8D2). Energy dispersive spectroscopy (EDS) was performed to detect the Ca/P ratio of the regenerated minerals in the CHX-PAM-ACP group. The molar ratio was 1.65, close to that of hydroxyapatite.

4. Discussion

The structure of G4-PAMAM-COOH includes three main components: core, inner repeating unit, and peripheral functional groups. The ^1H NMR spectrum showed the main structure of PAMAM was not changed after drug loading. The CHX may be either incorporated into PAMAM dendrimers via encapsulation within the core structure or attached to the peripheral functional groups via electrostatic interactions [26]. Because it is slightly soluble in water and positively charged. Although the mechanism of the interaction between CHX and PAMAM remains unproven, the CHX loaded dendrimers showed less cytotoxicity and more MMP inhibiting

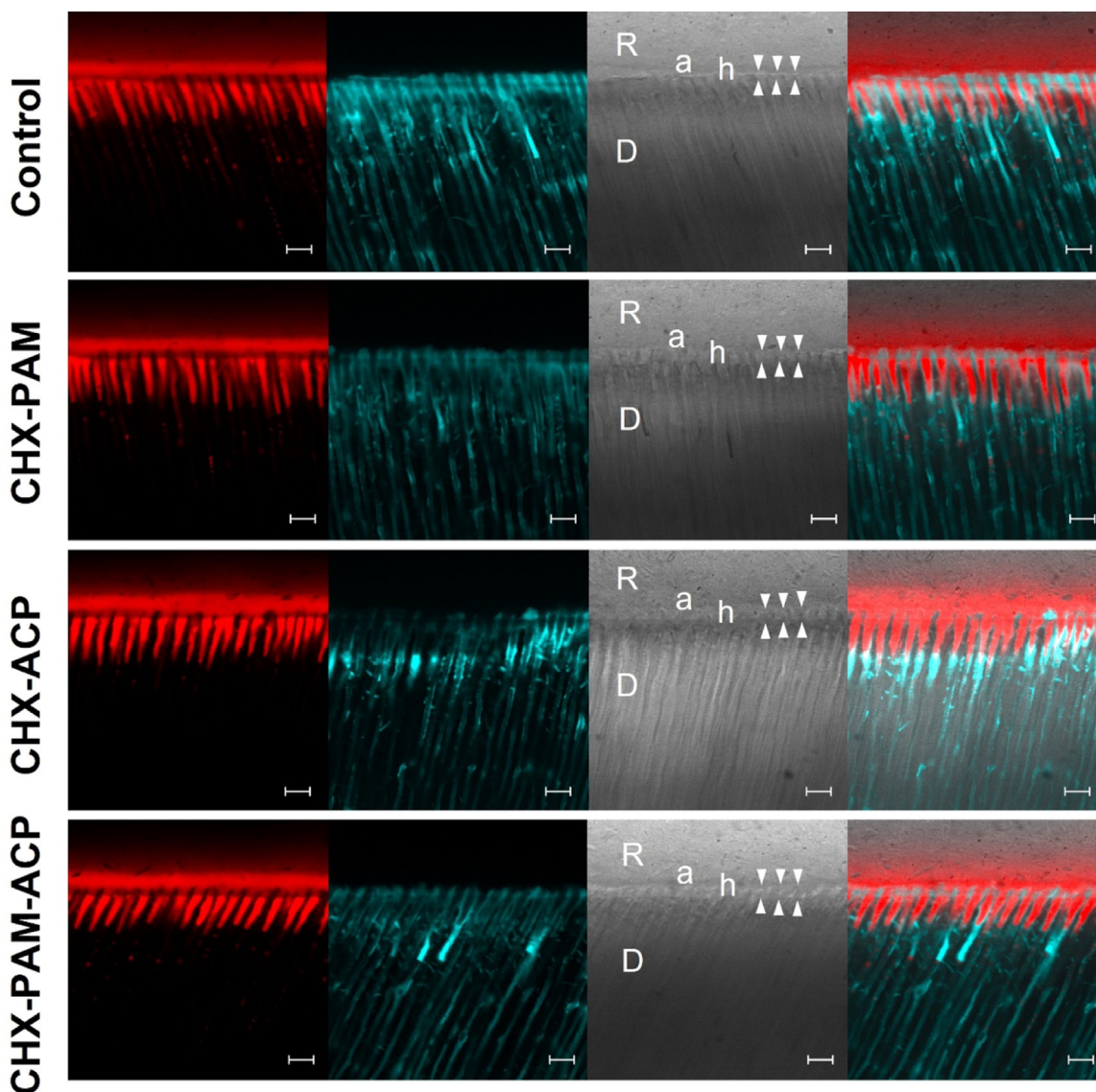


Fig. 7 – Representative confocal laser scanning microscopy images (Bar = 10 μm) demonstrating the permeability characteristics of the resin-dentin interfaces in the four groups. Left: Red channel of adhesive resin mixed with red fluorescent dye. Middle (left): Blue channel showing dye-containing water applied at 20 cm of water pressure from the pulpal side across the resin-dentin interface. Middle (right): Differential interference contrast images showing the optical density of the resin-dentin interface. Right: Merged channel. (R, resin composite; a, adhesive; h, hybrid layer between arrowheads; D, mineralized dentin).

properties after drug loading compared with the 0.2 wt% CHX solution.

The cytotoxicity increased as the components diffused over time in the control, CHX-PAM, and CHX-PAM-ACP groups, mainly because of the base materials of the PBE adhesive that was contained in all the groups. The addition of PAMAM dendrimers and ACP nanoparticles did not increase the cytotoxicity. As proven in previous studies, the 4th generation PAMAM dendrimers are non-toxic and non-immunogenic [38]. ACP is a natural precursor in the mineralization procedure, so it cannot be cytotoxic. In contrast, the cell viabilities of the CHX-ACP group were significantly less than the other groups in both cycles. The

cytotoxicity of the 0.2 wt% CHX cannot be easily ignored because the sample elution used in this study had already been diluted. This result is consistent with previous studies that demonstrate CHX concentrations greater than 0.2 wt% have a cytotoxic effect [16,19,39]. Priyadarshini et al. used Poly(ϵ -caprolactone) nanocapsules to encapsulate CHX and successfully reduced the cytotoxicity [40]. PAMAM dendrimers in this study also had a similar effect after drug loading. The reduction in cytotoxicity may improve the potentiality of clinical application on deep caries close to the pulp. The loading procedure may enhance the residence time of CHX within the hybrid layers and change the release mode [38].

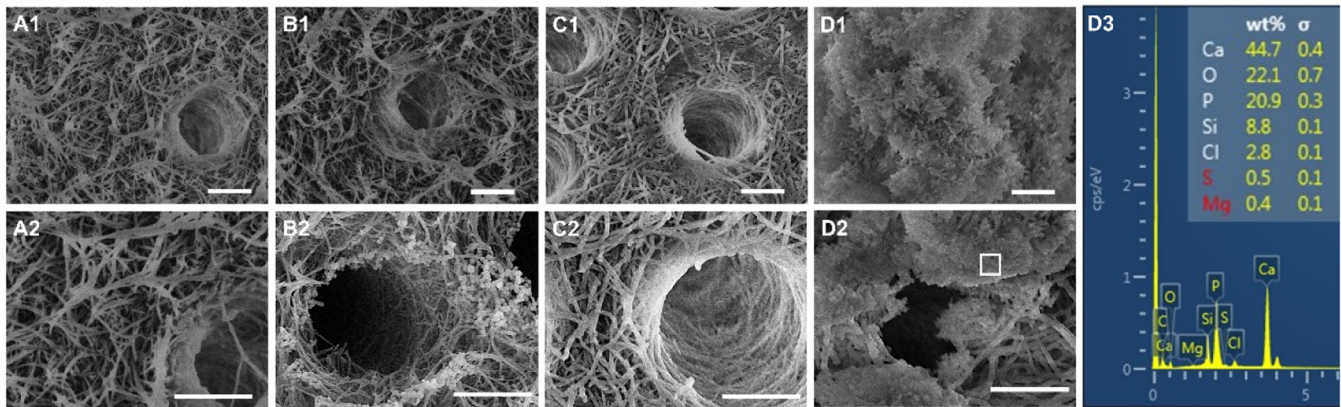


Fig. 8 – Representative SEM images (Bar = 2 μ m) of demineralized dentin treated with the four methods after 28 days reaction. (A1, A2) The Control group sample perpendicular to the dentinal tubule axis. (B1, B2) The CHX-PAM group sample. (C1, C2) The CHX-ACP group sample. The peritubular collagen fibrils were still exposed in B1–C2. (D1, D2) The CHX-PAM-ACP group sample showing needle-like minerals precipitated around dentinal tubules. (D3) EDS spectrum of the rectangular area in D2.

A relevant result was also observed using in situ zymography. After TMC, the CHX-PAM and CHX-PAM-ACP groups presented less MMPs activity than the CHX-ACP group. The molecular weight of CHX is 897 Da, which alone cannot be retained in the collagen fibrils. PAMAM dendrimers can be retained within the collagen fibrils via the size exclusion effect. After drug loading, more CHX may be preserved in the dentin matrix than CHX solution without PAMAM. Then, during incubation, CHX gradually separated from PAMAM and released into the interfibrillar area, inhibiting the activity of adjacent endogenous MMPs [26]. Therefore, a greater inhibitory effect on the activity of endogenous MMPs can be achieved. The latest research indicated PAMAM-NH₂ and PAMAM-COOH had additional effect on the inhibition of MMPs [24,41]. But another research, in which the methods were more similar to this study, found that PAMAM-COOH had no effect on the activity of dentin-bound MMPs [26]. It probably due to the different experimental methods. The roles of PAMAM in these studies were different as pretreatment agent or raw material of mineralization. When PAMAM used for mineralization, it may be fixed in the dentin matrix and difficult to interact with endogenous MMPs [26]. Further studies may need to make the mechanisms clear. However, the differences in anti-MMP experiment did not affect the μ TBS in the present study. The three groups containing CHX (CHX-PAM, CHX-ACP, CHX-PAM-ACP) all had greater μ TBS than the control after TMC. There was no significant difference among them, likely because the hydrolysis of hybrid layers take time after the activation of MMPs. The reduction of bond strength did not synchronize with the activation of the MMPs.

ACP nanoparticles can readily flow into dentinal tubules with adhesive to form resin tags [32]. The higher the ACP nanofiller concentration of the adhesive, the more Ca and P ions that can be released [33]. However, large amounts of fillers may have side effects on the integrity of the adhesive layer; the agglomeration of nanofillers may break off the adhesive layer, especially within the small-scale resin tags. In this study, the concentration of ACP nanoparticles reached 20 wt%. Although it was less than some previous work [31], it

was still a relatively high level of fillers for adhesives. PBE was chosen as the adhesive base because it uses acetone as an organic solvent. Acetone has a higher vapor pressure than ethanol, resulting in rapid solvent evaporation and less retention of residual water because of less vapor pressure reduction in organic solvent-water mixtures [42]. Furthermore, the permeability of the resin-dentin interfaces created by the experimental methods were also tested besides the immediate μ TBS. ACP nanofillers did not change the permeability of the interfaces created by PBE.

The remineralization effect of PAMAM dendrimers has been proven in many studies that were conducted in saliva-like solutions with Ca and P ions and a stable buffered pH [27,43,44]. The anionic carboxylic terminates of G4-PAMAM-COOH, after coating for 1–12 h [26,31], can attract Ca and P ions in an artificial saliva solution to form ACP precursors and arrange them in an ordered manner, resulting in crystallization [25]. This study also proved that remineralization could not be achieved without PAMAM (CHX-ACP group) or Ca/P ions (CHX-PAM group). Both substances must exist to induce mineralization. During this process, the only Ca and P source was the ACP-containing adhesive. The ions released from ACP-containing adhesive was sustained for longer than 30 days. The release was estimated to last longer than 2 years in the oral environment [34]. The molar ratio of Ca/P had an upward tendency after 14 days in our study. It might because the released Ca and P ions reacted as the environmental pH changed. The ions buffered the environment and serve as the raw materials with PAMAM for mineralization at the same time, which is consistent with a previous study [31]. The application time for PAMAM accompanied by brushing was reduced to 40 min in this study. Brushing may promote the contact between PAMAM and demineralized collagen fibrils. Further reduction of operating time will improve its potential for clinical use.

However, there are inevitable limitations of the present in vitro study. The better methods to simulate the in-vivo aging process are needed. Animal studies are also required to support the potential clinical application.

5. Conclusion

Within the limitations of the present study, it can be concluded that the novel method effectively enhanced bonding durability. G4-PAMAM-COOH dendrimers acted as both carriers to encapsulate/release CHX and a biomimetic analog to induce remineralization with the ACP-containing adhesive. The loaded CHX presented reduced cytotoxicity and inhibited MMP activities within hybrid layers to maintain μ TBS after TMC.

Acknowledgments

The authors declare no conflict of interest associated with the present study. The study was supported by the National Natural Science Foundation of China [grant number 51602008]. We thank Liwen Bianji (Edanz) for editing the English text of a draft of this manuscript.

REFERENCES

- [1] Gu LS, Cai X, Guo JM, Pashley DH, Breschi L, Xu HHK, et al. Chitosan-based extrafibrillar demineralization for dentin bonding. *J Dent Res* 2019;98(2):186–93.
- [2] Breschi L, Mazzoni A, Ruggeri A, Cadenaro M, Di Lenarda R, De, et al. Dental adhesion review: aging and stability of the bonded interface. *Dent Mater* 2008;24(1):90–101.
- [3] Tjaderhane L, Nascimento FD, Breschi L, Mazzoni A, Tersariol IL, Geraldeli S, et al. Strategies to prevent hydrolytic degradation of the hybrid layer – a review. *Dent Mater* 2013;29(10):999–1011.
- [4] Huang B, Siqueira WL, Cvitkovitch DG, Finer Y. Esterase from a cariogenic bacterium hydrolyzes dental resins. *Acta Biomater* 2018;71:330–8.
- [5] Gou YP, Meghil MM, Pucci CR, Breschi L, Pashley DH, Cutler CW, et al. Optimizing resin-dentin bond stability using a bioactive adhesive with concomitant antibacterial properties and anti-proteolytic activities. *Acta Biomater* 2018;75:171–82.
- [6] Mazzoni A, Scaffa P, Carrilho M, Tjäderhane L, Di Lenarda R, Polimeni A, et al. Effects of etch-and-rinse and self-etch adhesives on dentin MMP-2 and MMP-9. *J Dent Res* 2013;92(1):82–6.
- [7] Frassetto A, Breschi L, Turco G, Marchesi G, Di Lenarda R, Tay FR, et al. Mechanisms of degradation of the hybrid layer in adhesive dentistry and therapeutic agents to improve bond durability – a literature review. *Dent Mater* 2016;32(2):e41–53.
- [8] Wu Z, Wang X, Wang Z, Shao C, Jin X, Zhang L, et al. Self-etch adhesive as a carrier for ACP nanoprecursors to deliver biomimetic remineralization. *ACS Appl Mater Interfaces* 2017;9(21):17710–7.
- [9] Tao S, He L, Xu HHK, Weir MD, Fan M, Yu Z, et al. Dentin remineralization via adhesive containing amorphous calcium phosphate nanoparticles in a biofilm-challenged environment. *J Dent* 2019;89:103193.
- [10] Fan M, Zhang M, Xu HHK, Tao S, Yu Z, Yang J, et al. Remineralization effectiveness of the PAMAM dendrimer with different terminal groups on artificial initial enamel caries in vitro. *Dent Mater* 2020;36(2):210–20.
- [11] Yang J, Cao S, Li J, Xin J, Chen X, Wu W, et al. Staged self-assembly of PAMAM dendrimers into macroscopic aggregates with a microribbon structure similar to that of amelogenin. *Soft Matter* 2013;9(31):7553.
- [12] Li J, Yang J, Li J, Chen L, Liang K, Wu W, et al. Bioinspired intrafibrillar mineralization of human dentine by PAMAM dendrimer. *Biomaterials* 2013;34(28):6738–47.
- [13] Liu Y, Tjaderhane L, Breschi L, Mazzoni A, Li N, Mao J, et al. Limitations in bonding to dentin and experimental strategies to prevent bond degradation. *J Dent Res* 2011;90(8):953–68.
- [14] Stanislawczuk R, Pereira F, Muñoz MA, Luque I, Farago PV, Reis A, et al. Effects of chlorhexidine-containing adhesives on the durability of resin–dentine interfaces. *J Dent* 2014;42(1):39–47.
- [15] Verma UP, Gupta A, Yadav RK, Tiwari R, Sharma R, Balapure AK. Cytotoxicity of chlorhexidine and neem extract on cultured human gingival fibroblasts through fluorescence-activated cell sorting analysis: an in-vitro study. *Eur J Dent* 2018;12(3):344–9.
- [16] Liu JX, Werner J, Kirsch T, Zuckerman JD, Virk MS. Cytotoxicity evaluation of chlorhexidine gluconate on human fibroblasts, myoblasts, and osteoblasts. *J Bone Jt Infect* 2018;3(4):165–72.
- [17] Breschi L, Mazzoni A, Nato F, Carrilho M, Visintini E, Tjaderhane L, et al. Chlorhexidine stabilizes the adhesive interface: a 2-year in vitro study. *Dent Mater* 2010;26(4):320–5.
- [18] Lin J, Kern M, Ge J, Zhu J, Wang H, Vollrath O, et al. Influence of peripheral enamel bonding and chlorhexidine pretreatment on resin bonding to dentin. *J Adhes Dent* 2013;15(4):351–9.
- [19] Brunello G, Becker K, Scotti L, Drescher D, Becker J, John G. The effects of three chlorhexidine-based mouthwashes on human osteoblast-like saos-2 cells. *Vitr Study Int J Mol Sci* 2021;22(18):9986.
- [20] Sadek FT, Braga RR, Muench A, Liu Y, Pashley DH, Tay FR. Ethanol wet-bonding challenges current anti-degradation strategy. *J Dent Res* 2010;89(12):1499–504.
- [21] Wang Y, Guo R, Cao X, Shen M, Shi X. Encapsulation of 2-methoxyestradiol within multifunctional poly(amidoamine) dendrimers for targeted cancer therapy. *Biomaterials* 2011;32(12):3322–9.
- [22] Abbasi E, Aval SF, Akbarzadeh A, Milani M, Nasrabadi HT, Joo SW, et al. Dendrimers: synthesis, applications, and properties. *Nanoscale Res Lett* 2014;9(1):1–10.
- [23] Toroian D, Lim JE, Price PA. The size exclusion characteristics of type I collagen. *J Biol Chem* 2007;282(31):22437–47.
- [24] Gou Y, Jin W, He Y, Luo Y, Si R, He Y, et al. Effect of cavity cleanser with long-term antibacterial and anti-proteolytic activities on resin–dentin bond stability. *Front Cell Infect Mi* 2021;11:784153.
- [25] Zhou Y, Yang J, Lin Z, Li J, Liang K, Yuan H, et al. Triclosan-loaded poly(amido amine) dendrimer for simultaneous treatment and remineralization of human dentine. *Colloids Surf B: Biointerfaces* 2014;115:237–43.
- [26] Chen L, Chen W, Yu Y, Yang J, Jiang Q, Wu W, et al. Effect of chlorhexidine-loaded poly(amido amine) dendrimer on matrix metalloproteinase activities and remineralization in etched human dentin in vitro. *J Mech Behav Biomed Mater* 2021;121:104625.
- [27] Tay FR, Pashley DH. Guided tissue remineralisation of partially demineralised human dentine. *Biomaterials* 2008;29(8):1127–37.
- [28] Gu LS, Kim YK, Liu Y, Takahashi K, Arun S, Wimmer CE, et al. Immobilization of a phosphonated analog of matrix phosphoproteins within cross-linked collagen as a templating mechanism for biomimetic mineralization. *Acta Biomater* 2011;7(1):268–77.
- [29] Wang Q, Wang XM, Tian LL, Cheng ZJ, Cui FZ. In situ remineralization of partially demineralized human dentine mediated by a biomimetic non-collagen peptide. *Soft Matter* 2011;7(20):9673.

- [30] Liang K, Xiao S, Shi W, Li J, Yang X, Gao Y, et al. 8DSS-promoted remineralization of demineralized dentin in vitro. *J Mater Chem B Mater Biol Med* 2015;3(33):6763–72.
- [31] Liang K, Xiao S, Weir MD, Bao C, Liu H, Cheng L, et al. Poly (amido amine) dendrimer and dental adhesive with calcium phosphate nanoparticles remineralized dentin in lactic acid. *J Biomed Mater Res B Appl Biomater* 2017;106(6):2414–24.
- [32] Zhang L, Weir MD, Hack G, Fouad AF, Xu HH. Rechargeable dental adhesive with calcium phosphate nanoparticles for long-term ion release. *J Dent* 2015;43(12):1587–95.
- [33] Chen C, Weir MD, Cheng L, Lin NJ, Lin-Gibson S, Chow LC, et al. Antibacterial activity and ion release of bonding agent containing amorphous calcium phosphate nanoparticles. *Dent Mater* 2014;30(8):891–901.
- [34] Chen C, Weir MD, Cheng L, Lin NJ, Lin-Gibson S, Chow LC, et al. Antibacterial activity and ion release of bonding agent containing amorphous calcium phosphate nanoparticles. *Dent Mater* 2014;30(8):891–901.
- [35] Perote LC, Kamozaki MB, Gutierrez NC, Tay FR, Pucci CR. Effect of matrix metalloproteinase-inhibiting solutions and aging methods on dentin bond strength. *J Adhes Dent* 2015;17(4):347–52.
- [36] Pucci CR, Gu L, Zhang H, Song Q, Xia VW, Davis LB, et al. Water-associated attributes in the contemporary dentin bonding milieu. *J Dent* 2018;74:79–89.
- [37] Cai X, Han B, Liu Y, Tian F, Liang F, Wang X. Chlorhexidine-loaded amorphous calcium phosphate nanoparticles for inhibiting degradation and inducing mineralization of type I collagen. *ACS Appl Mater Interfaces* 2017;9(15):12949–58.
- [38] Cerofolini L, Baldoneschi V, Dragoni E, Storai A, Mamusa M, Berti D, et al. Synthesis and binding monitoring of a new nanomolar PAMAM-based matrix metalloproteinases inhibitor (MMPIs). *Bioorgan Med Chem* 2017;25(2):523–7.
- [39] Sukumaran SK, Vadakkekuttikal RJ, Kanakath H. Comparative evaluation of the effect of curcumin and chlorhexidine on human fibroblast viability and migration: an in vitro study. *J Indian Soc Periodo* 2020;24(2):109–16.
- [40] Priyadarshini BM, Selvan ST, Lu TB, Xie H, Neo J, Fawzy AS. Chlorhexidine nanocapsule drug delivery approach to the resin-dentin interface. *J Dent Res* 2016;95(9):1065–72.
- [41] Wu Q, Shan T, Zhao M, Mai S, Gu L. The inhibitory effect of carboxyl-terminated polyamidoamine dendrimers on dentine host-derived matrix metalloproteinases in vitro in an etch-and-rinse adhesive system. *R Soc Open Sci* 2019;6(10):182104.
- [42] Zhang Z, Tian F, Niu L, Ochala K, Chen C, Fu B, et al. Defying ageing: an expectation for dentine bonding with universal adhesives? *J Dent* 2016;45:43–52.
- [43] Gu LS, Kim YK, Liu Y, Takahashi K, Arun S, Wimmer CE, et al. Immobilization of a phosphonated analog of matrix phosphoproteins within cross-linked collagen as a templating mechanism for biomimetic mineralization. *Acta Biomater* 2011;7(1):268–77.
- [44] Zhou YZ, Cao Y, Liu W, Chu CH, Li QL. Polydopamine-induced tooth remineralization. *ACS Appl Mater Interfaces* 2012;4(12):6901–10.